ELSEVIER

Journal of Molecular Graphics and Modelling 21 (2002) 57–70

Journal of Molecular Graphics and Modelling

www.elsevier.com/locate/JMGM

A semiempirical study on the electronic structure of 10-deacetylbaccatin-III

S.F. Braga, D.S. Galvão*

Instituto de Física Gleb Wataghin, Universidade Estadual de Campinas, UNICAMP, CP 6165, CEP 13091-970, Campinas, SP, Brazil

Abstract

We performed a conformational and electronic analysis for 10-deacetylbaccatin-III (DBAC) using well-known semiempirical methods (parametric method 3 (PM3) and Zerner's intermediate neglect of differential overlap (ZINDO)) coupled to the concepts of total and local density of states (LDOS). Our results indicate that regions presented by paclitaxel (Taxol®) as important for the biological activity can be traced out by the electronic features present in DBAC. These molecules differ only by a phenylisoserine side chain. Compared to paclitaxel, DBAC has a simpler structure in terms of molecular size and number of degrees of freedom (d.f.). This makes DBAC a good candidate for a preliminary investigation of the taxoid family. Our results question the importance of the oxetane group, which seems to be consistent with recent experimental data.

Keywords: Paclitaxel; Taxoids; Baccatin; Semiempirical methods; Molecular orbital calculations

1. Introduction

Cancer is a general term covering hundreds of related diseases. They are characterized by cellular growth accumulating genetic alterations as they progress to a more malignant phenotype [1]. It is believed that cancers are a consequence of a combination of complex factors related to heredity, lifestyle and environment [2–4]. Cancer is nowadays the second major cause of human death in industrialized countries [5].

These death rates have been significantly reduced in the last decades due in part to the successful use of chemotherapeutic agents [4]. The search for new or more potent drugs presenting fewer side effects is a continuous challenge to pharmaceutical researchers. Among the new families of these drugs, the natural product paclitaxel (Taxol®/Bristol-Myers-Squibb) and its derivative docetaxel (Taxotere®/Rhone-Poulenc Rorer) are probably the most promising antitumor agents under investigation [6–8]. FDA approved paclitaxel for use in the treatment of advanced ovarian cancer in 1992 and 1994 for the treatment of breast cancer. Today other pharmaceutical companies such as the Korean Samyang Genex [9] and the Canadian IVAX Corporation [10] are marketing these drugs.

Paclitaxel has a unique mechanism of action, it blocks cancer cell division by promoting the polymerization and stabilization of protein tubulin to microtubules and inhibits the depolymerization of microtubules back to tubulin. This is the opposite effect of other antimitotic agents like vinca alkaloids, which prevent microtubule assembly [11,12].

Unfortunately, despite paclitaxel's remarkable biological activity, its use in large scale has been limited due to its poor availability from natural sources. Paclitaxel is a natural product isolated from the bark of the western Pacific yew tree, *Taxus Brevifolia* [13] which has to be cut down to extract the drug. The bark from two trees barely give enough compound to treat a single patient [14]. One practical answer to this problem was the partial synthesis from 10-deacetylbaccatin-III (DBAC), a natural substance isolated from the leaves of the *Taxus* species [12]. The leaves are a renewable natural resource, and the DBAC is isolated in abundance.

The synthetic product docetaxel was obtained by the Institute de Chimie des Substances Naturelles in 1981, during a semi-synthetic route to paclitaxel [15]. Significant progress toward the total synthesis for Taxol® have been achieved in the last decade [16–19]. This offers new possibilities in terms of drug availability.

Considering the topological structures, DBAC (Fig. 1) and paclitaxel (Fig. 2) differ only by a phenylisoserine side chain. This chain is essential for the antitumor activity of the taxoid family, which is characterized by the diterpene core [20,21]. DBAC has 39 heavy atoms while paclitaxel has 60.

* Corresponding author. Tel.: +55-19-3788-5369; fax: +55-19-3788-5376.
E-mail address: galvao@ifi.unicamp.br (D.S. Galvão).

1093-3263/02/$ – see front matter
PII: S1093-3263(02)00121-3

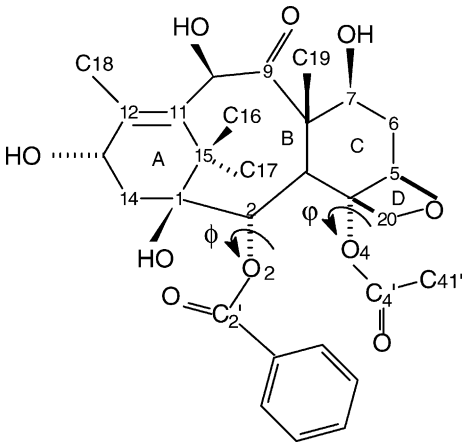

Fig. 1. Structural representation of DBAC. The dihedral angles ϕ and φ are defined by the atoms C1–C2–O2–C2′ and C5–C4–O4–C4′, respectively.

Compared to paclitaxel, DBAC has a simpler structure in terms of molecular size and number of degrees of freedom (d.f.). This makes DBAC a good candidate for a preliminary investigation of the taxoid family.

The regions of the groups benzoate, acetate and oxetane (Fig. 2), are considered as biologically important to the antitumor activity presented by paclitaxel and derivatives. The benzoate and acetate seem to be necessary to allow binding to tubulin in the human body. The oxetane is necessary for bioactivity, but it is not clear whether it is involved in the binding or just serves as a conformational lock [22].

The development of new drugs is a very timely and costly process. The costs of synthesis and biological testing sometimes make it difficult to bring a new product to market. Theoretical approaches that can a priori select between good or bad candidates can be very effective for reducing costs and time requirements. Structure-activity relationship (SAR) studies can offer essential information suggesting and identifying geometric and electronic features related to biological activity. Surprisingly, in spite of the obvious importance of taxoids, only a few theoretical studies [23–29] have been carried out on these structures.

In this work, we report a geometric and spectroscopic theoretical study for DBAC. We have fully characterized its geometry, conformational configuration space and simulated absorption spectra using well-known semiempirical methods. We have also investigated the possible correlation between regions of biological importance (benzoate, acetate and oxetane) and electronic and spectroscopic features.

2. Methodology

Paclitaxel and DBAC are large and very flexible molecules. Their sizes and the necessity to carry out detailed conformational analysis preclude the use of ab initio quantum mechanical methods. However, semiempirical molecular orbital calculations are feasible. Semiempirical methods such as modified neglect of differential overlap (MNDO) [30], Austin method 1 (AM1) [31] and parametric method 3 (PM3) [32–34] provide a good balance between quality and computational effort, and they have been successfully used to treat many organic compounds [35].

The AM1 method was developed in an attempt to correct some of the MNDO weaknesses. In AM1, as in the MNDO, all the two-center nuclear attraction integrals are retained,

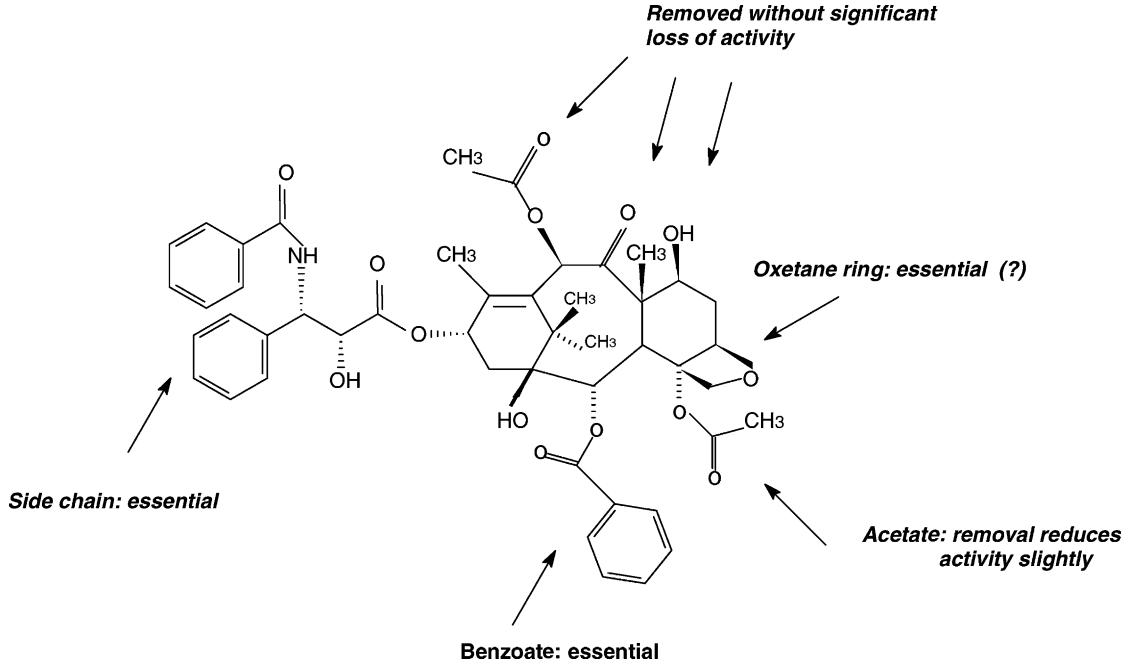

Fig. 2. Structural representation of paclitaxel (Taxol®). The relevant regions for the biological activity are also indicated. Adapted from [9].

but the tendency of MNDO to overestimate the repulsion between atoms has been corrected by a suitable modification of the core repulsion function [31]. A more recent formulation of these methods—the PM3—was introduced to improve on MNDO and AM1 results. PM3 differs from AM1 in that the former treats the one-center, two-electron integrals as pure parameters, as opposed of being derived from atomic spectroscopy. In PM3, all quantities that enter the Fock matrix and the total energy expression have been treated as pure parameters [35].

However, although it seems to be a consensus that AM1 and PM3 are general better than MNDO, there is an ongoing debate about the relative merits of the two methods. Some studies are in favor of PM3 [36–43] and some of AM1 [44–46].

In the present work, we have carried out some tests in order to decide between AM1 and PM3. We compare the predicted AM1 and PM3 DBAC geometries against X-ray data available for related compounds and conclude that the PM3 is the better choice (see Section 3 for details).

DBAC presents two major flexible groups, benzoate and acetate (Fig. 1). We have carried out a systematic conformational search varying simultaneously the dihedral angles defining these groups (Fig. 1). These calculations were performed using the Chem2Pac [47] program. Chem2Pac allows automatic two-dimensional conformational searches using the MOPAC 6 package [34] that contains the PM3 hamiltonian.

Chem2Pac is a free software package developed at our group for the Windows™ operating system of a personal computer. It allows automatic conformational searches and also contains a recent version of LDOS methodology [48,49] that will be discussed later.

Since we have to handle many structures and we are interested in analyzing electronic and spectroscopic features over specific molecular regions, one fast and efficient way to do this is to explore the concepts of DOS and LDOS. The electronic DOS is defined as the number of electronic states per energy unit. The related concept of LDOS, i.e. the DOS calculated over a specific molecular region, is introduced in order to describe the spatial distribution of these states as well.

The PM3 hamiltonian is a Hartree–Fock method based on the linear combination of atomic orbitals (LCAO) approximation [50]

$$\psi_m = \sum_i C_{mi}\varphi_i \tag{1}$$

where ψ refers to the molecular orbitals, φ to the atomic ones and C_{mi} are the expansion coefficients.

For the LDOS calculations, the contribution of each atom to an electronic level is weighted by the square of the (real) molecular orbital coefficient, i.e. by the probability density corresponding to the level in that site. The summation is carried over the selected molecular regions, that is, over the selected atomic orbitals (from n_i to n_f), leading to the following expression [48]:

$$\mathrm{LDOS}(E_i) = 2\sum_{m=n_i}^{n_f} |C_{mi}|^2 \tag{2}$$

The factor 2 comes from the Pauli exclusion principle (maximum of 2 electrons per electronic level). This is a discrete modulation, which allows a direct comparison of DOS and LDOS calculated from any LCAO method.

The LDOS method permits us to map the distribution of any molecular orbital, occupied or virtual, over the molecular skeleton. In other words, LDOS shows how an atom or a set of them contribute to the formation of the specified molecular orbitals. The LDOS approach has some advantages over conventional three-dimensional rendering MO contours, such as: cheaper computational cost, easiness to analyze, simultaneous determinations of relative contribution from various molecular levels, and results without resolution plot dependence.

These LDOS calculations can be easily performed in an automatic way using the Chem2Pac program [47]. The DOS and LDOS concepts have been recently used to identify active and inactive compounds in several different classes of organic compounds including carcinogens, [48,49,51] antibiotics, [52] hormones, [53,54] and HIV protease inhibitors [55].

Geometrical features such as bond lengths, bond angles, dihedral angles as well as heats of formation (H.F.), dipole moment values, etc. are well described by PM3, but the electronic transitions are overestimated, as expected from a zero differential overlap (ZDO) method without configuration interaction (CI) corrections. Thus, in order to have a more realistic description of the electronic transitions, i.e. to simulate the absorption spectra, it is necessary to use methods specially developed to handle these aspects. We have chosen the Zerner's intermediate neglect of differential overlap-spectroscopic (ZINDO/S-CI) method in a version specially calibrated to study organic compounds [56,57]. We have carried out ZINDO/S-CI calculations using on average 200 configurations (singlet/triplet) with the geometries obtained from PM3 calculations. We have used the Mataga–Nishimoto approach for the gamma integrals with the usual interaction factors [57] of 1.267 and 0.585. The average ZINDO errors [35] are only 1000–2000 cm^{-1} ($\sim$0.1–0.2 eV) for all bands $<$45 000 cm^{-1}. This methodology (PM3 geometries for ZINDO/S-CI calculations) has been used with success in the description of organic molecules [38,39,58,59]. The simulated absorption spectra are generated by Lorentzian enveloping (half-width of 0.03 eV) the ZINDO/S-CI transition energies weighted by the oscillator strength values [59].

3. Results and discussions

As mentioned in Section 2 in order to decide between the semiempirical methods PM3 and AM1, we have carried out some tests.

Although there are no X-ray data for DBAC, X-ray analysis for a similar compound has been reported in the literature [60]: 2′-carbamate paclitaxel (CTAX, Fig. 3). CTAX has essentially the same tetracyclic ring system (TRS) present in DBAC, paclitaxel and docetaxel [29]. It is believed that the geometry of the TRS can be considered as a rigid structure [61–65]. Density functional theory (DFT) results [29] have been reported for the DBAC, which contains the same TRS group present in our molecule. We use the TRS experimental geometric data to compare the predicted AM1, PM3 and DFT geometries.

Because a detailed conformational search is cost prohibitive at the DFT level, [29] the DFT predicted structure was obtained using a small number of minima with geometries generated using the experimental X-ray data as a guide. In order to benchmark our AM1 and PM3 results, we have used the same procedure.

In Table 1, we present the results for some relevant bond lengths, angles and dihedrals. In Table 2, we present the overall RMS deviations comparing PM3, AM1 and DFT

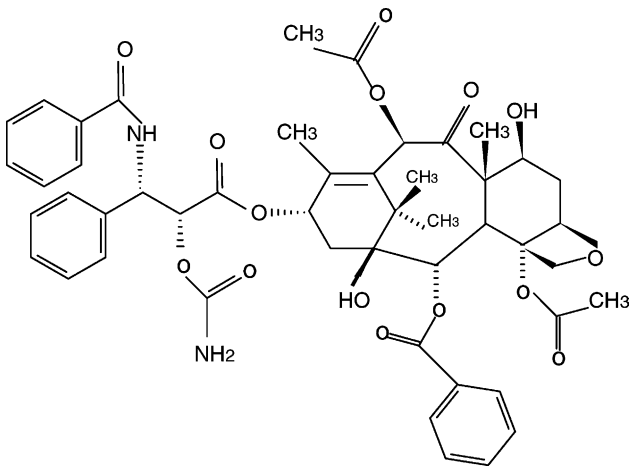

Fig. 3. Structural representation of 2′-CTAX.

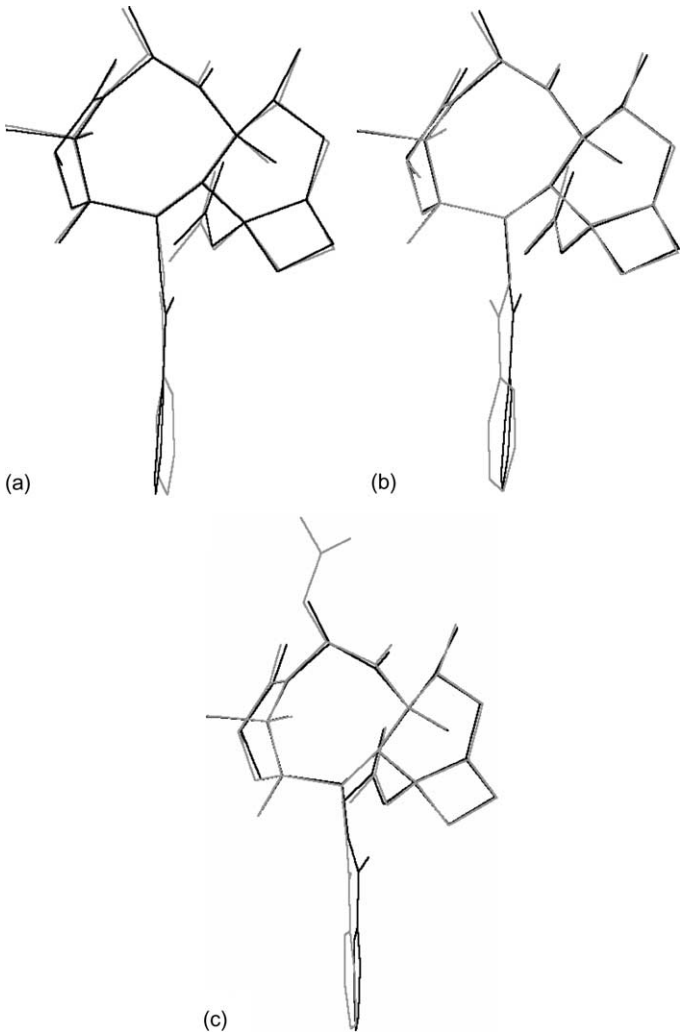

Fig. 4. Superimposed calculated geometrical structures and X-ray data (darker): (a) PM3; (b) AM1; (c) DFT.

Table 1
Relevant bond lengths, angles and dihedrals (see text for discussions)

Atoms	X-ray	PM3	AM1	DFT	BC	Atoms	X-ray	PM3	AM1	DFT	BC
(a) Bond length (Å)											
O1–C1	1.424	1.422	1.427	1.452	1.424	C1–C15	1.564	1.577	1.554	1.570	1.577
O2–C2	1.452	1.430	1.442	1.473	1.430	C2–C3	1.565	1.570	1.543	1.575	1.572
O2–C21	1.358	1.369	1.373	1.364	1.372	C3–C4	1.547	1.553	1.532	1.560	1.552
O4–C4	1.455	1.432	1.430	1.477	1.435	C3–C8	1.564	1.563	1.543	1.588	1.561
O4–C41	1.359	1.366	1.371	1.366	1.362	C4–C5	1.542	1.585	1.574	1.559	1.585
O5–C5	1.467	1.457	1.461	1.480	1.457	C4–C20	1.534	1.572	1.566	1.540	1.570
O5–C20	1.427	1.442	1.452	1.464	1.441	C5–C6	1.528	1.516	1.504	1.522	1.515
O7–C7	1.440	1.407	1.415	1.435	1.407	C6–C7	1.526	1.528	1.520	1.531	1.529
O9–C9	1.212	1.222	1.239	1.221	1.217	C7–C8	1.585	1.567	1.559	1.588	1.566
O10–C10	1.443	1.411	1.42	1.463	1.405	C8–C9	1.547	1.549	1.533	1.568	1.559
O13–C13	1.458	1.416	1.428	1.459	1.406	C8–C18	1.546	1.531	1.525	1.541	1.531
O21–C21	1.202	1.219	1.236	1.229	1.214	C9–C10	1.524	1.543	1.527	1.549	1.546
O41–C41	1.206	1.216	1.233	1.224	1.217	C10–C11	1.503	1.505	1.497	1.503	1.508
C11–C15	1.535	1.511	1.505	1.539	1.512	C11–C12	1.345	1.352	1.353	1.356	1.353
C12–C19	1.498	1.487	1.480	1.506	1.484	C12–C13	1.515	1.512	1.506	1.525	1.513
C15–C16	1.559	1.540	1.535	1.553	1.544	C13–C14	1.524	1.543	1.532	1.542	1.544
C41–C42	1.490	1.502	1.490	1.507	1.504	C15–C17	1.548	1.540	1.527	1.544	1.535
C1–C2	1.567	1.605	1.568	1.580	1.600	C21–C22	1.481	1.488	1.470	1.492	1.490
C1–C14	1.557	1.546	1.536	1.549	1.552						
(b) Angle (°)											
C2–O2–C21	116.4	119.9	118.2	118.6	119.8	O4–C4–C3	108.7	110.6	110.2	109.5	110.4
C4–O4–C41	117.2	122.4	119.9	117.1	121.9	O4–C4–C5	113.3	112.7	111.8	112.0	112.4
C5–O5–C20	91.5	93.7	93.3	90.9	93.6	O4–C4–C20	108.6	105.1	106.1	108.5	105.3
O1–C1–C14	110.2	104.4	104.1	104.6	108.4	C3–C4–C5	119.2	120.4	120.6	119.7	120.7
O1–C1–C15	107.8	109.7	109.8	109.9	110.1	C3–C4–C20	120.5	121.0	120.7	119.9	121.2
C2–C1–C14	111.3	112.3	111.0	112.6	112.2	C5–C4–C20	84.7	84.1	84.8	85.2	84.1
C2–C1–C15	111.4	110.5	112.2	112.4	111.3	O5–C5–C4	90.5	91.4	90.6	90.7	90.3
C14–C1–C15	111.1	112.3	112.7	110.7	111.5	O5–C5–C6	113.6	111.6	112.0	112.7	111.7
O2–C2–C1	104.9	106.2	105.4	104.8	105.3	C4–C5–C6	120.3	118.2	119.0	120.3	117.9
O2–C2–C3	109.0	109.0	107.6	107.9	109.9	C5–C6–C7	113.3	111.6	110.7	113.9	111.4
C1–C2–C3	118.5	116.9	116.3	119.5	116.6	C12–C13–C14	112.2	110.7	112.4	112.7	110.2
O7–C7–C6	106.7	110.6	110.9	110.0	110.4	C1–C14–C13	115.4	115.0	116.1	117.5	115.3
O7–C7–C8	109.5	113.1	111.6	113.8	113.2	C1–C15–C11	105.5	104.7	105.7	105.8	104.7
C6–C7–C8	110.7	112.1	111.6	112.8	112.1	C1–C15–C16	110.5	109.2	110.8	110.5	110.1
C3–C8–C7	104.8	107.4	106.6	105.5	107.7	C1–C15–C17	110.8	113.3	111.5	110.7	112.9
C3–C8–C9	115.4	115.3	116.2	117.8	115.2	C11–C15–C16	110.8	109.4	110.2	115.9	109.5
C3–C8–C18	113.2	110.1	112.3	112.9	110.0	C11–C15–C17	116.3	116.9	114.8	109.9	116.5
C7–C8–C9	102.4	104.0	104.0	102.2	104.2	C16–C15–C17	103.0	103.7	104.0	104.1	103.4
C7–C8–C18	113.7	112.9	110.5	111.2	112.5	O5–C20–C4	92.4	91.4	91.3	92.1	91.5
C9–C8–C18	107.0	107.1	106.8	106.6	107.3	O2–C21–O21	123.3	119.2	118.6	123.9	120.5
O9–C9–C8	119.9	120.7	119.4	119.6	119.2	O2–C21–C22	111.6	114.1	113.5	111.5	112.5
C8–C9–C10	119.3	124.7	122.4	120.8	122.4	O21–C21–C22	125.1	126.7	127.9	124.7	127
O10–C10–C9	109.9	110.7	111.8	108.6	112.9	C9–C10–C11	114.3	111.9	112.4	114.4	112.2
O10–C10–C11	110.8	111.3	108.8	110.3	112.1	C10–C11–C15	120.8	121.4	119.3	119.6	120.7

Table 1 (*Continued*)

Atoms	X-ray	PM3	AM1	DFT	BC	Atoms	X-ray	PM3	AM1	DFT	BC
C10–C11–C12	118.7	119.5	121.0	120.6	120.4	C11–C12–C13	116.7	118.8	119.0	118.9	118.4
C12–C11–C15	119.7	118.8	119.4	119.5	118.7	C13–C12–C19	117.3	117.8	116.5	115.8	117.4
C11–C12–C19	126.0	123.3	124.4	125.3	124.2	O4–C41–O41	122.7	120.6	119.1	123.5	121.0
C2–C3–C4	113.6	114.7	112.6	111.3	114.8	O4–C41–C42	109.7	111.9	112.2	110.9	112.6
C2–C3–C8	114.2	112.0	114.0	115.9	112.2	O41–C41–C42	127.6	127.4	128.7	125.7	126.5
C4–C3–C8	111.0	111.5	111.5	111.0	111.5						
(c) Dihedral (°)											
C1–C2–C3–C4	−125.8	−123.1	−127.3	−132.2	−124.1	O1–C1–C2–O2	53.3	46.9	53.9	55.9	50.5
C1–C2–C3–C8	105.6	108.5	104.5	99.65	107.5	C6–C5–O5–C20	130.6	115.8	123.8	131.4	115.1
C1–C2–O2–C21	−104.3	−96.0	−86.3	−93.7	−103.5	C6–C7–C8–C18	51.4	51.2	49.1	53.2	51.2
C2–C3–C4–C5	−154.6	−154.3	−151	−154.4	−153.7	C6–C7–C8–C9	166.4	166.9	163.4	166.6	167.1
C2–C3–C4–C20	−52.6	−51.9	−47.8	−51.9	−51.1	C6–C5–C4–C20	−124.4	−110.4	−117.5	−124.6	−110.1
C2–C3–C4–O4	73.6	71.5	76.3	74.4	72.4	C7–C8–C9–O9	−104.8	−97.7	−96.7	−96.1	−98.8
C2–C3–C8–C7	−171.1	−178.3	−179.1	−175.3	−179.2	C7–C8–C9–C10	66.7	76.3	74.1	74.9	75.2
C2–C3–C8–C9	−59.2	−62.9	−63.7	−62.0	−63.5	C8–C9–C10–O10	−171.1	−179.1	−179.2	179.9	−172.9
C3–C2–O2–C21	127.9	137.2	148.9	137.9	130.2	C9–C10–C11–C12	−123.2	−118.8	−122.8	−122.6	−123
C3–C4–C5–C6	−2.4	12.0	5.2	−2.8	12.8	C18–C8–C9–O9	15.0	22.0	20.3	20.7	20.6
C3–C4–C20–O5	−114.3	−126.7	−120.9	−114.0	−127.5	O7–C7–C8–C18	−65.9	−74.6	−75.7	−73.1	−74.5
C3–C4–C5–O5	115.5	127.2	120.9	114.3	127.7	C9–C10–C11–C15	46.9	55.3	50.8	50.9	52.1
C3–C4–O4–C41	79.5	78.8	75.8	77.4	76.9	O9–C9–C10–O10	0.5	−4.7	−8.2	−8.99	1.1
C3–C8–C7–O7	169.9	163.8	162.0	164.1	164.3	O10–C10–C11–C15	−77.9	−69.2	−73.5	−72.0	−76.0
C3–C8–C7–C6	−72.7	−70.4	−73.2	−69.7	−70.1	C10–C11–C12–C13	164.8	168.4	163.6	166.8	168.4
C4–C5–C6–C7	−8.8	−26.1	−21.4	−6.99	−27.3	C10–C11–C15–C16	7.5	1.3	4.1	2.3	2.6
C4–O4–C41–O41	−1.8	0.2	−1.4	−3.2	2.7	C10–C11–C15–C17	124.6	118.6	121.1	120.0	119.5
C4–O4–C41–C42	178.6	180.3	178.9	176.4	183.4	C10–C11–C15–C1	−115.6	−119.7	−119.2	−120.5	−119.2
C2–O2–C21–O21	−9.0	−6.4	−6.5	−4.2	−14.5	C10–C11–C12–C19	−13.6	−8.4	−12.3	−12.1	−10.4
C2–O2–C21–C22	172.6	174.6	175.1	176.2	167.1	C11–C12–C13–O13	−159.3	−161.9	−151.9	−152.9	−168.7
O2–C21–C22–C23	9.4	6.4	0.9	−3.25	56	C11–C12–C13–C14	−42.1	−41.7	−34.6	−34.4	−42.1
O2–C21–C22–C27	−170.9	−173.4	−178.8	175.8	−125	C11–C15–C1–C14	−53.9	−54.9	−53.5	−56.2	−54.8
C5–C6–C7–O7	165.4	183.4	181.0	172.1	184.1	C11–C15–C1–O1	−174.7	−170.6	−169.1	−171.3	−175.1
C5–C6–C7–C8	46.4	56.2	55.7	43.86	56.9	C11–C15–C1–C2	70.7	71.2	72.6	70.6	71.3
C2–C3–C8–C18	64.5	58.5	59.7	63.1	57.9	C12–C13–C14–C1	36.9	35.8	30.7	26.3	37.6
C4–C3–C8–C18	−65.6	−71.7	−69.2	−65.2	−72.2	C12–C11–C15–C16	177.5	175.4	177.8	176.1	177.8
C4–C3–C8–C7	58.9	51.6	52.0	56.5	50.6	C12–C11–C15–C17	−65.4	−67.2	−65.2	−66.2	−65.3
C4–C3–C8–C9	170.8	167	167.4	169.7	166.4	C12–C11–C15–C1	54.3	54.5	54.5	53.3	56.1
C5–C4–C3–C8	−24.3	−25.6	−21.5	−23.7	−24.9	O13–C13–C12–C19	19.3	15.0	24.3	26.1	10.2
C5–C4–O4–C41	−55.5	−59.2	−61.2	−57.8	−61.1	C14–C1–C2–C3	55.9	54.5	60.3	62.9	56.3
C13–C14–C1–C15	11.6	12.0	13.5	19.2	10.5	C14–C1–C2–O2	−65.9	−67.4	−58.8	−58.1	−65.9
O13–C13–C14–C1	159.3	161.2	152.4	149.3	166.2	O1–C1–C15–C16	58.7	63.4	65.6	62.5	58.9
C13–C14–C1–O1	130.9	130.7	132.4	137.5	131.8	O1–C1–C15–C17	−54.8	−51.5	−49.8	−52.3	−56.1
C14–C1–C15–C16	179.4	179.0	181.2	177.6	179.3	C20–C4–O4–C41	−147.8	−149.1	−152	−150.1	−150.9
C14–C1–C15–C17	65.9	64.1	65.8	62.8	64.9						

Table 2
Overall RMS comparing the different methods against experimental X-ray data

RMS			
	Bond length (Å)	Angle (°)	Dihedral (°)
X-ray × PM3	0.117	16.59	53.86
X-ray × AM1	0.514	15.1	53.57
X-ray × DFT	0.499	3.78	6.67

versus the available X-ray data. In Fig. 4, we present the theoretical predicted structures superimposed against those obtained from X-ray data. We can see that the general geometric features are well described by all methods. From Table 1 and Fig. 4, we conclude that the PM3 method produced better geometrical data than AM1. Based on this, we have chosen PM3 to carry out our DBAC conformational investigations. It is interesting to notice that PM3 produced better bond lengths than DFT.

The results of our systematic conformational search indicated that the procedure of generating structures using X-ray

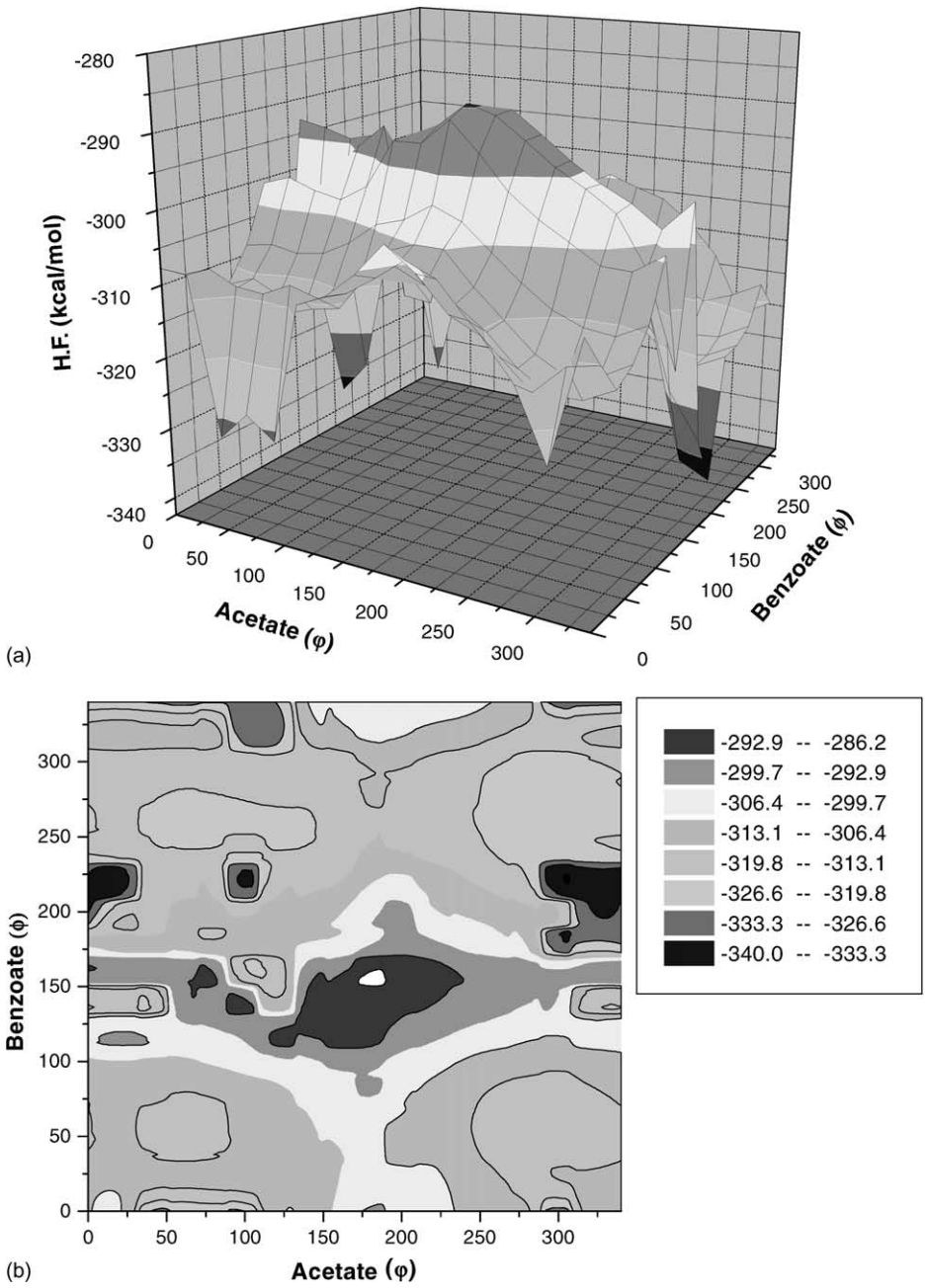

Fig. 5. (a) Three-dimensional representation of the energy surface space for benzoate (ϕ) and acetate (φ) group rotations. See Fig. 1 for angle definition; (b) two-dimensional contour plot of Fig. 3 (a).

data as a guide could be misleading. Our results showed that the optimized structures obtained in this way are, in fact, in local minima. We have located PM3 conformers more than 1 kcal/mol lower in energy. In Table 1, we also present the geometrical data for best (lowest energy) conformer obtained from systematic search. As can be seen from Table 1, there are significant differences for some dihedral angles. For molecules presenting this kind of conformational complexity, a systematic conformational search must be performed. Due to the computational costs semiempirical methods remains the best option.

In Fig. 5, we present the results for the systematic conformational search, varying simultaneously the dihedral angles ϕ and φ (Fig. 1) from 0 to 360° in steps of 20°. This is an important search to reliably locate the global minimum as well as possible conformations thermally accessible in the temperature range of the human body.

As we can see from Fig. 5, the conformational space is a very rich one, with many valleys and hills. One interesting feature is the existence of many minima associated with the acetate group rotation while for the benzoate rotations between 25 and 75°, there are no minima. This is related to steric impediments as illustrated in Fig. 6. For this angle region, the oxygen atom from the benzoate group becomes closer to the carbon C20 from the oxetane ring (darker atoms in Fig. 6), and there is a steric hindrance to this movement with a consequent increase in the total energy.

In our conformational analysis, we have considered 324 conformers (Fig. 1). In order to have an estimate of the thermally accessible conformers, we have calculated the Boltzmann population (B.P.) distribution at room temperature (300 K). In Table 3, we present the 10 most stable conformers from the conformational grid and the associated B.P. As we can see from the table, the first five conformers correspond

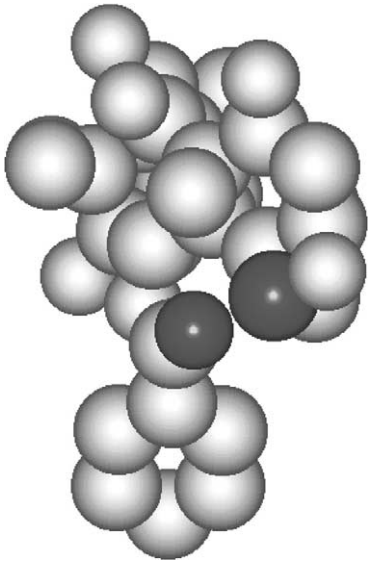

Fig. 6. Three-dimensional overlapping spheres rendering of DBAC. See text for discussions.

Table 3
Results for the B.P. analysis

Conformer	φ	ϕ	ΔE	B.P.
1	300	220	0	0.43
2	340	220	0.033	0.40
3	320	220	0.863	0.10
4	20	220	1.132	0.06
5	0.0	220	2.689	5.0×10^{-1}
6	100	220	3.899	5.9×10^{-4}
7	0.0	200	4.444	2.5×10^{-4}
8	320	200	5.804	2.5×10^{-5}
9	340	200	6.562	7.0×10^{-6}
10	300	180	6.718	5.4×10^{-6}

See text for discussions.

to 99% of the population distribution. These conformers are associated to wide rotations of the φ angle, while the ϕ angle remains essentially the same. From the systematic grid, the most probable structures for the absolute minimum are identified. Full geometric optimization calculations were then carried out for them and the best conformer (BC) obtained.

We then proceed with the LDOS calculations for the BC and the structures indicated in Table 3. We have analyzed in detail three major molecular regions (Fig. 1): the skeleton (composed by the regions A, B, C and D), the acetate and benzoate groups. Typical LDOS results are displayed in Fig. 7. One major advantage of the LDOS calculations is to allow the simultaneous determination of the relative contribution to each molecular level of the chosen molecular regions. Using this procedure, we can easily map the spatial distribution of the relevant molecular levels (in general the frontier orbitals).

An analysis of the electronic effects due to acetate and benzoate group rotations for the BC showed that these rotation barriers are high, but the changes in the ionization potential (IP) values are not significant (∼0.2 eV). The dipole moment values present significant variation as expected from the presence of highly polar molecular regions.

We have analyzed separately the benzoate and acetate rotations, by keeping one of the two major flexible groups at its optimum value and varying the other in steps of 30°. The LDOS results showed that the frontier orbitals are concentrated over the skeleton and benzoate regions. We did not observe relevant contributions to these orbitals from the acetate and oxetane regions. The benzoate rotations produce little change in the frontier orbitals. The acetate rotations produce significant variations only for the LUMO + 1.

The main contributions of atomic orbitals for HOMO formation come from the skeleton region, more specifically from the atoms of the rings A and B (Fig. 1). We observe a localization of the HOMO − 1 and LUMO orbitals over the benzoate ring, more concentrated over phenol group. The LUMO+1 is more sensible to the benzoate and acetate rotations. We observe a pattern for the acetate's spatial orientations. Configurations for which the oxygen of acetate is near the oxetane group (D ring) have the L + 1 orbital distributed

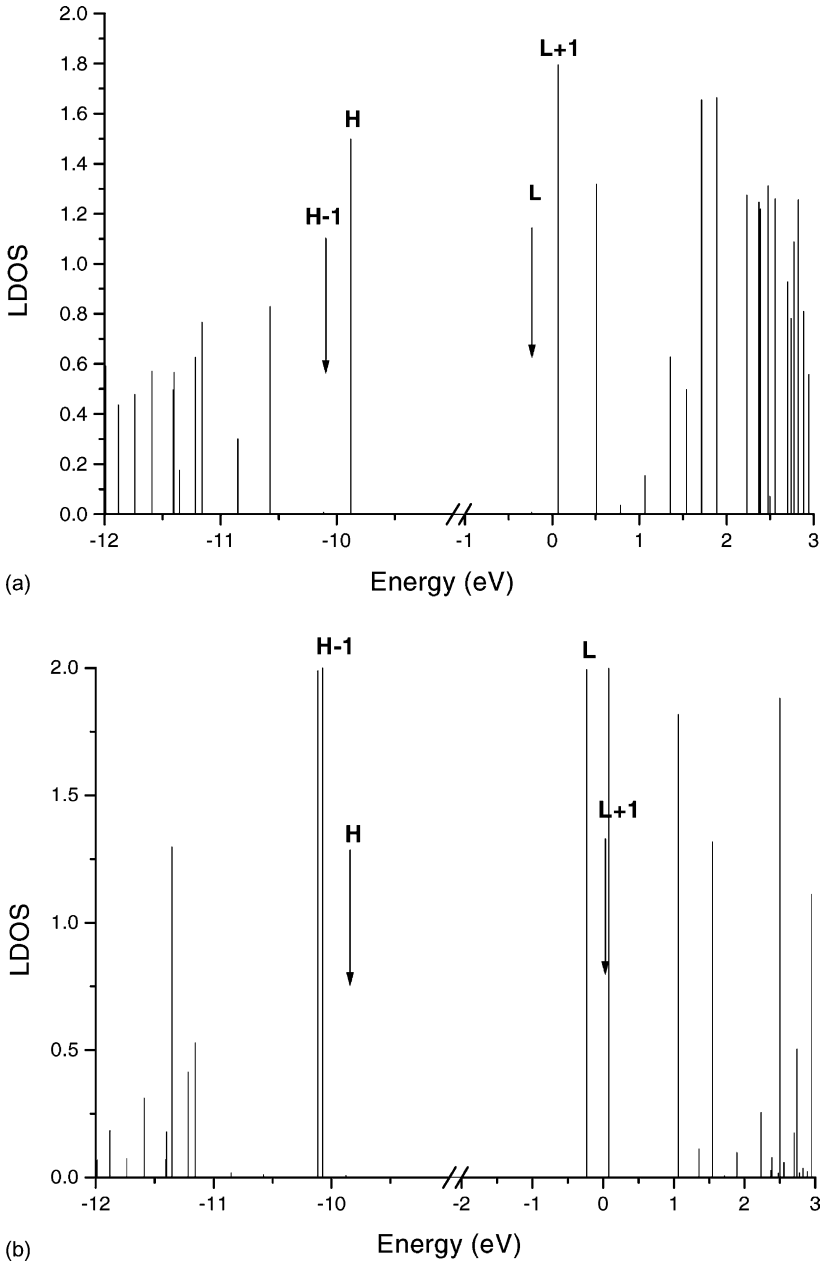

Fig. 7. Typical LDOS for: (a) skeleton region; (b) benzoate group. For clarity only some of occupied and virtual molecular levels are displayed. Each vertical line in the graphic represents the contribution from a specific region (skeleton or benzoate) to the formation of the molecular orbital at that specific energy level. H and L refer to the HOMO and LUMO, respectively.

over the A- and B-ring of molecular skeleton, while for the remaining configurations the orbitals are concentrated over the ring phenol of the benzoate group.

The LDOS analysis provides a very fast and practical way to determine the molecular orbital spatial distributions. It produces the same level of information as obtained from the more usual and costly three-dimensional orbital rendering (Fig. 8).

In Table 4, we present some electronic, structural and LDOS results for the 10 most stable conformers from the B.P. analysis. For comparison, the results for the BC are also indicated. We can see from Table 4 that there are small variations for the dipole and IP values for the Boltzmann conformers when compared to the BC. The LDOS patterns for these conformers (with relation to the φ and ϕ values) are very similar to those observed for the BC.

The results permit us to understand the experimentally observed relative importance of some regions for the paclitaxel's biological activity. Benzoate, acetate, oxetane and some side groups attached to the skeleton (Fig. 2) are

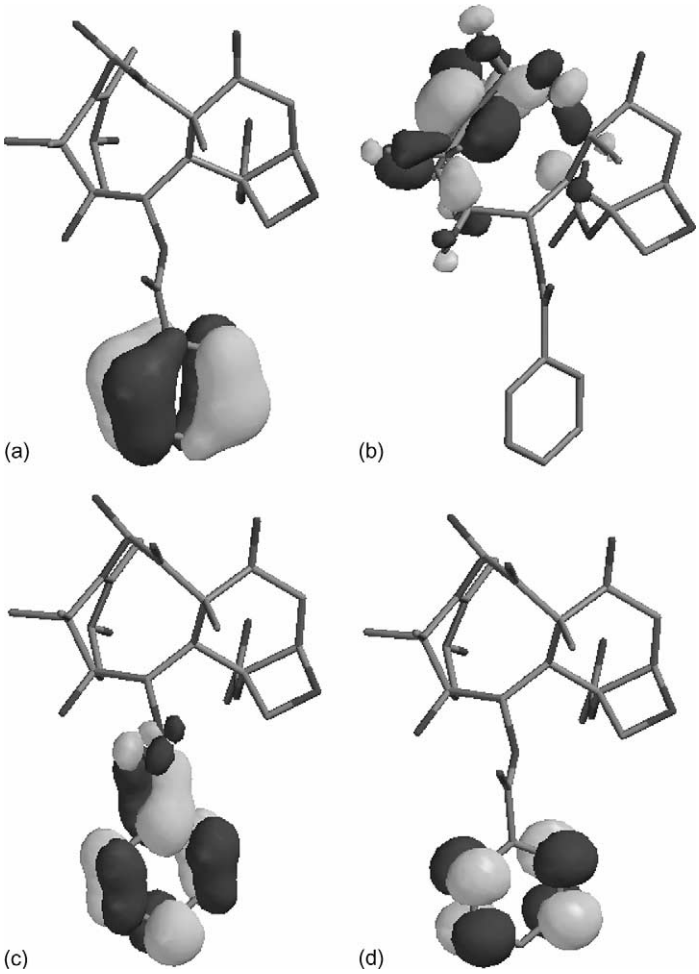

Fig. 8. Typical three-dimensional rendering of molecular orbitals: (a) HOMO − 1; (b) HOMO; (c) LUMO; (d) LUMO + 1.

considered as essential to the biological activity. All these regions, with the exception of oxetane, are exactly the important regions (in electronic terms) observed for DBAC. This suggests that the importance of these groups can be traced by the DBAC's electronic structure. The oxetane is reported in the literature [11] as being essential to the paclitaxel's biological activity, but our results show that it does not actively participate in the frontier orbitals formation. As pointed out by Wang et al. [66] while a number of studies have reinforced the biological importance of the side chains (hydrophobic collapse) the role of the oxetane has been more speculative. Two hypothesis have been considered; direct participation in the rigidicity of the paclitaxel core (favoring conformational locking) or, alternatively,

Table 4
PM3 results for H.F., dipole moment, IP and spatial distribution for the frontier orbitals

Conformer	H.F.	Dipole	IP	φ	ϕ	Skeleton	Benzoate
BC	−345.63	5.51	9.85	299	256	H	H − 1, L, L + 1
1	−338.35	4.27	9.78	300	220	H	H − 1, L, L + 1
2	−338.32	5.51	9.93	340	220	H, L + 1	H − 1, L
3	−337.49	4.25	9.77	320	220	H	H − 1, L, L + 1
4	−337.22	5.90	9.89	20	220	H, L + 1	H − 1, L
5	−335.66	4.55	9.84	0	220	H, L + 1	H − 1, L
6	−334.45	4.46	9.89	100	220	H, L + 1	H − 1, L
7	−333.91	5.46	9.91	0	200	H, L + 1	H − 1, L
8	−332.55	4.30	9.79	320	200	H	H − 1, L, L + 1
9	−331.79	4.50	9.82	340	200	H, L + 1	H − 1, L
10	−331.63	5.18	9.86	300	180	H	H − 1, L, L + 1

lowering the dipole–dipole interactions facilitating tubulin binding. However, recent studies by Wang et al. [66] have questioned the oxetane's importance. They have shown that taxol analogues present bioactivity without the presence of oxetane group. Our electronic analysis are consistent with these experimental results and support conclusions that oxetane group is not essential to the biological activity of taxoids.

With the PM3 geometries, we carried out ZINDO-S/CI calculations in order to investigate the nature of the excited states. We have simulated the absorption spectra, analyzing the effects of ring rotations to the optical spectra. We have also determined (from the CI coefficients) the relative importance of some geometrical regions associated to the molecular levels involved in the electronic excited states.

In Table 5 and Fig. 9, we present the summary of the ZINDO results and the simulated absorption spectra for the BC and the Boltzmann's conformers. We observed that the main features (threshold absorption and maximum absorption values) are not very sensitive to group rotations (about 3.4 and 6.9 eV, respectively), while the main CI contributions (Table 5) are more sensitive to these rotations. The analysis of the CI contributions provides dynamic (electronic excitation) complementary information to LDOS results. From the CI coefficients, it is possible to identify the molecular orbitals involved in a specific electronic transition. From the spatial distribution of these states (which could be obtained from the LDOS calculations), it is possible to identify the geometric molecular regions important to this specific transition. This information can be used as a guide to structural changes in order to maintain or to alter this optical transition.

The main electronic contributions to the threshold and the strongest absorptions are shown in Table 5. The notation [A → B] means a configuration generated taking one electron from the molecular orbital A and putting it in the molecular orbital B. The predominant configurations for threshold absorptions are mainly formed by the transition involving electrons from orbitals H − 4, H − 3 and H to orbitals L + 1 and L + 5. For the maximum absorption, the main contributions are from electrons from H − 1, H − 2 to the L and L + 4 orbitals.

The most important chromophore in the diterpenoid moiety of taxoids is the enone system. For DBAC carbonyl, benzoate, and olefinic chromophores are present. Experimental UV data showed anomalous absorption band at 275–285 nm, as well bathochromic shifts [67]. From our simulated absorption spectra, the first significant absorption and the maxima are around 5.2 and 6.8 eV (Fig. 9), respectively. They compare well with the available experimental data [26,67,68] of 5.2 eV (230 nm) and 6.5 eV (285 nm), respectively.

The results for DBAC encourage us to apply the present methodology to the more challenging investigation of taxol derivatives trying to identify electronic molecular descriptors capable of classifying active and inactive compounds. This is a demanding computer analysis, but preliminary results [69] are encouraging.

In summary, we have presented here a conformational and electronic analysis of DBAC combining the use of semiempirical methods with the total and LDOS concepts.

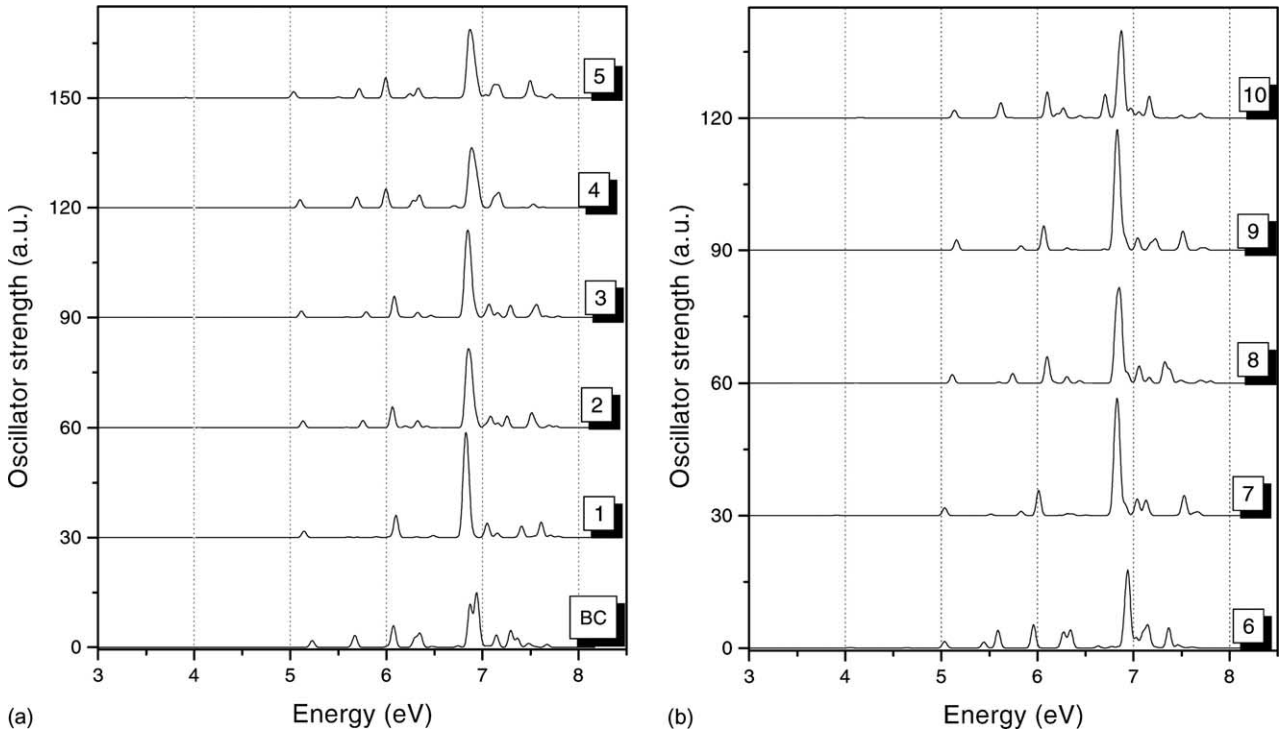

Fig. 9. Typical ZINDO simulated absorption spectra: (a) and (b).

Table 5
Energy, oscillator strengths and main CI contributions to the absorption threshold (first transition) and the highest peak (maximun absorption) for ZINDO simulated absorption spectra

Conformers	Threshold absorption (eV)/(cm^{-1})	Oscillator strength (a.u.)	Main contributions	Maximum absorption (eV)/(cm^{-1})	Oscillator strength (a.u.)	Main contributions
BC	3.44/27748.9	0.0013	$0.829[H-3\rightarrow L+3]-0.456[H-3\rightarrow L+5]-0.196[H\rightarrow L+3]+0.101[H\rightarrow L+5]$	6.94/55932.8	0.7309	$0.555[H-2\rightarrow L+4]+0.452[H-1\rightarrow L+2]+0.339[H-1\rightarrow L+9]+0.330[H-1\rightarrow L+4]$
1	3.48/28064.7	0.0020	$0.621[H-3\rightarrow L+2]-0.565[H-3\rightarrow L+1]+0.388[H-3\rightarrow L+5]-0.207[H\rightarrow L+2]$	6.81/54942.3	1.0197	$-0.509[H-1\rightarrow L]+0.715[H-2\rightarrow L+3]-0.248[H-4\rightarrow L]+0.215[H-1\rightarrow L+4]$
2	3.48/28043.3	0.0018	$-0.559[H-3\rightarrow L+1]-0.494[H-4\rightarrow L+1]-0.315[H-3\rightarrow L+5]-0.280[H-4\rightarrow L+5]$	6.88/55485.5	0.8459	$0.531[H-1\rightarrow L+3]+0.519[H-2\rightarrow L+4]-0.358[H-1\rightarrow L+9]-0.315[H-2\rightarrow L]$
3	3.48/28088.7	0.0020	$0.654[H-3\rightarrow L+2]-0.535[H-3\rightarrow L+1]+0.391[H-3\rightarrow L+5]+0.223[H\rightarrow L+2]$	6.83/55085.2	0.9592	$0.649[H-2\rightarrow L+3]+0.406[H-1\rightarrow L+4]-0.379[H-1\rightarrow L]-0.221[H-4\rightarrow L]$
4	3.44/27713.1	0.0007	$0.608[H-3\rightarrow L+2]+0.414[H-4\rightarrow L+2]-0.413[H-3\rightarrow L+5]-0.283[H-4\rightarrow L+5]$	6.91/55745.1	0.5816	$-0.494[H-1\rightarrow L+9]+0.491[H-2\rightarrow L+4]-0.410[H-1\rightarrow L+3]+0.300[H-2\rightarrow L+3]$
5	3.46/27906.7	0.0016	$0.779[H-4\rightarrow L+1]-0.388[H-4\rightarrow L+5]-0.291[H-3\rightarrow L+1]-0.281[H\rightarrow L+1]$	6.86/55296.0	0.8560	$-0.596[H-2\rightarrow L+3]-0.476[H-1\rightarrow L+4]-0.328[H-1\rightarrow L]-0.269[H-5\rightarrow L]$
6	3.40/27422.8	0.0010	$0.794[H-4\rightarrow L+1]+0.369[H\rightarrow L+1]+0.364[H-3\rightarrow L+2]+0.214[H-4\rightarrow L+4]$	6.86/55296.0	0.8560	$-0.596[H-2\rightarrow L+3]-0.476[H-1\rightarrow L+4]-0.328[H-1\rightarrow L]-0.269[H-5\rightarrow L]$
7	3.46/27875.2	0.0015	$0.719[H-4\rightarrow L+1]+0.382[H-4\rightarrow L+5]-0.283[H-3\rightarrow L+1]-0.292[H-4\rightarrow L]$	6.84/55196.3	1.0404	$0.663[H-1\rightarrow L+3]-0.494[H-2\rightarrow L]-0.443[H-2\rightarrow L+4]-0.187[H-2\rightarrow L+1]$
8	3.48/28031.0	0.0016	$0.660[H-3\rightarrow L+1]+0.525[H-3\rightarrow L+2]+0.390[H-3\rightarrow L+5]-0.229[H\rightarrow L+1]$	6.82/55005.3	0.8554	$-0.643[H-2\rightarrow L+3]-0.367[H-1\rightarrow L]+0.396[H-1\rightarrow L+4]-0.286[H-4\rightarrow L]$
9	3.47/28009.3	0.0005	$0.633[H-3\rightarrow L+1]-0.466[H-3\rightarrow L+5]+0.414[H-3\rightarrow L+2]+0.218[H-4\rightarrow L+1]$	6.81/54937.4	0.9491	$0.696[H-2\rightarrow L+3]-0.442[H-1\rightarrow L]-0.331[H-1\rightarrow L+4]-0.281[H-5\rightarrow L]$
10	3.47/28018.6	0.0014	$0.621[H-3\rightarrow L+1]-0.503[H-3\rightarrow L+2]+0.392[H-3\rightarrow L+5]+0.233[H\rightarrow L+2]$	6.88/55500.7	0.9494	$-0.606[H-2\rightarrow L+4]-0.576[H-1\rightarrow L+3]+0.306[H-2\rightarrow L]+0.244[H-2\rightarrow L+3]$

Using this methodology, we have identified the relative importance (in terms of electronic features) of specific DBAC's molecular regions (Fig. 2). Our results indicate that regions that are considered important for the biological activity of taxol can be traced by the electronic features already present in DBAC. The same results question the biological importance of the oxetane group, which seems to be consistent with recent experimental data reported by Wang et al. [66].

Acknowledgements

The authors acknowledge the financial support from the Brazilian Agencies FAPESP and CNPq.

References

[1] T. Sugimura, Multistep carcinogenesis: a 1992 perspective, Science 258 (1992) 603–607.
[2] R.G. McKinnel (Ed.), The Biological Basis of Cancer, Cambridge University Press, Cambridge, 1998.
[3] H. Lodish, D. Baltimore, A. Berk, S.L. Zipursky, P.M. Sudaira, J. Darnell, Molecular cell biology, in: Scientific American Books, 3rd edition, New York, 1995.
[4] R.W. Ruddon (Ed.), Cancer Biology, Oxford University Press, New York, 1987.
[5] EIU Marketing in Europe, Trade Reviews, 337, December 1990.
[6] G.I. Georg, G.C.B. Harriman, D.G.V. Velde, T.C. Boge, Z.S. Cheruvallath, A. Datta, M. Hepperle, H. Park, R.H. Himes, L. Jayasinghe, Medicinal chemistry of paclitaxel chemistry, strucutre-activity relationships, and conformational analysis, in: G.I. Georg, T.T. Chen, I. Ojima, D.M. Vyas (Eds.), Taxane Anticancer Agents, A.C.S. Symposium Series 583, American Chemical Society, Washington, DC, 1995, pp. 217–232.
[7] A. Commerçon, J.D. Bourzat, E. Didier, F. Lavelle, Practical semisynthesis and antimitotic activity of docetaxel and side-chain analogues, in: G.I. Georg, T.T. Chen, I. Ojima, D.M. Vyas (Eds.), Taxane Anticancer Agents, A.C.S. Symposium Series 583, American Chemical Society, Washington, DC, 1995, pp. 233–246.
[8] S.-H. Chen, V. Farina, Paclitaxel structure-activity relationships and core skeletal rearrangements, in: G.I. Georg, T.T. Chen, I. Ojima, D.M. Vyas (Eds.), Taxane Anticancer Agents, A.C.S. Symposium Series 583, American Chemical Society, Washington, DC, 1995, pp. 247–262.
[9] Samyang Pharmaceutical Business Division http://www.samyang.co.kr/english/news/news3.html.
[10] IVAX Corporation, http://www.ivax.com/.
[11] P. Jenkins, Taxol branches out, Chem. Brit. 11 (1996) 43–46.
[12] A. Stierle, D. Stierle, G. Strobel, G. Bignami, P. Grothaus, Bioactive metabolites of endophytic fungi of pacific yew, *Taxus Brevifolia*, paclitaxel, taxanes, and other bioactive compounds, in: G.I. Georg, T.T. Chen, I. Ojima, D.M. Vyas (Eds.), Taxane Anticancer Agents, A.C.S. Symposium Series 583, American Chemical Society, Washington, DC, 1995, pp. 81–97.
[13] S.J. Campbell, S.A. Whitney, The Pacific yew environmental impact statement, in: G.I. Georg, T.T. Chen, I. Ojima, D.M. Vyas (Eds.), Taxane Anticancer Agents, A.C.S. Symposium Series 583, American Chemical Society, Washington, DC, 1995, pp. 58–71.
[14] D. Guénard, F. Guéritte-Voegelein, P. Potier, Taxol and taxotere: discovery, chemistry, and structure-activity relationships, Acc. Chem. Res. 26 (1993) 160–167.
[15] F. Guéritte-Voegelein, D. Guénard, F. Lavelle, M.T. Le Goff, L. Mangatal, P. Potier, Relationships between the structure of taxol analogues and their antimitotic activity, J. Med. Chem. 34 (1991) 992–998.
[16] K.C. Nicolaou, Z. Yang, J.J. Lui, H. Ueno, P.G. Nantermet, R.K. Guy, C.F. Clalborne, J. Renaud, E.A. Couladouros, K. Paulvannan, E.J. Sorensen, K.C. Nicolaou, Z. Yang, J.J. Lui, H. Ueno, P.G. Nantermet, R.K. Guy, C.F. Clalborne, J. Renaud, E.A. Couladouros, K. Paulvannan, E.J. Sorensen, Total synthesis of taxol, Nature 367 (1994) 630–634.
[17] R.A. Holton, C. Somoza, H.B. Kim, F. Liang, R.J. Biediger, P.D. Boatman, M. Shindo, C.C. Smith, S. Kim, H. Nadizadeh, Y. Suzuki, C. Tao, P. Vu, S. Iang, P. Zlang, K.K. Muthi, L.N. Gentile, J.H. Lui, First total synthesis of taxol. Part 1. Functionalization of the B-ring, J. Am. Chem. Soc. 116 (1994) 1597–1598.
[18] R.A. Holton, C. Somoza, H.B. Kim, F. Liang, R.J. Biediger, P.D. Boatman, M. Shindo, C.C. Smith, S. Kim, H. Nadizadeh, Y. Suzuki, C. Tao, P. Vu, S. Iang, P. Zlang, K.K. Muthi, L.N. Gentile, J.H. Lui, First total synthesis of taxol. Part 2. Completion of the C- and D-ring, J. Am Chem. Soc. 116 (1994) 1599–1600.
[19] L. Wessjohann, The first total syntheses of taxol, Angw. Chem. Int. Edit. 33 (1994) 959–961.
[20] C.S. Swindell, N.E. Krauss, Biologically active taxol analogues with deleted A-ring side chain substituents and variable C-2′ configurations, J. Med. Chem. 34 (1991) 1176–1184.
[21] L.R. Jayasinghe, Structure-activity studies of antitumor taxanes: synthesis of novel C13 side chain homologated taxol and taxotere analogs, J. Med. Chem. 37 (1994) 2981–2984.
[22] M. Suffness, Overview of paclitaxel research: progress on many fronts, in: G.I. Georg, T.T. Chen, I. Ojima, D.M. Vyas (Eds.), Taxane Anticancer Agents, A.C.S. Symposium Series 583, American Chemical Society, Washington, DC, 1995, pp. 1–17.
[23] M. Lozynski, D. Rusinska-Roszak, PM3 conformations of C13 Taxol® side chain methyl ester, Tetrahedron Lett. 36 (1995) 8849–8852.
[24] H.J. Williams, G. Moyna, A.I. Scott, C.S. Swindell, L.E. Chirlian, J.M. Heerding, D.K. Williams, NMR and molecular modeling study of the conformations of taxol 2′-acetate in chloroform and aqueous dimethyl sulfoxide solutions, J. Med. Chem. 39 (1996) 1555–1559.
[25] M. Milanesio, P. Ungliengo, D. Viterbo, Ab initio conformational study of phenylisoserine side chain of paclitaxel, J. Med. Chem. 42 (1999) 291–299.
[26] H. Baumann, R.E. Martin, F. Diederich, PM3 geometry optimization and CNDO/S-CI computation of UV–VIS spectra of large organics structures: program description and application to poly(triacetylene) hexamer and taxotere, J. Comput. Chem. 20 (1999) 396–411.
[27] J.P. Snyder, N. Nevins, D.O. Cicero, J. Jansen, The conformations of taxol in chloroform, J. Am Chem. Soc. 122 (2000) 724–725.
[28] J.R. Cheeseman, G.W. Trucks, T.A. Keith, M.J. Frisch, A comparison of models for calculating nuclear magnetic resonance shielding tensor, J. Chem. Phys. 104 (1996) 5497–5509.
[29] P. Ballone, M. Marchi, A density functional study of a new family of anticancer drugs: paclitaxel, taxotere, epothilone, and discodermolide, J. Phys. Chem. A 103 (1999) 3097–3102.
[30] M.J.S. Dewar, M.L. McKee, Ground states of molecules. Part 41. MNDO results for molecules containing boron, J. Am. Chem. Soc. 99 (1977) 5231.
[31] M.J.S. Dewar, E.G. Zoebisch, E.F. Healy, J.J.P. Stewart, The development and use of quantum mechanical molecular models. Part 76. AM1—a new general purpose quantum mechanical molecular model, J. Am. Chem. Soc. 107 (1985) 3902.
[32] J.J.P. Stewart, Optimization of parameters for semiempirical methods 1, Method J. Comput. Chem. 10 (1989) 209–220.
[33] J.J.P. Stewart, Optimization of parameters for semiempirical methods. Part 2. Applications, J. Comput. Chem. 10 (1989) 221–264.
[34] MOPAC Program, Version 6.0, Quantum Chemistry Program Exchange No. 455. http://qcpe.chem.indiana.edu.

[35] M.C. Zerner, Semiempirical molecular orbital methods, in: K.B. Lipkowitz, D.B. Boyd (Eds.), Reviews in Computational Chemistry, VCH, New York, 1991, pp. 313–365.
[36] P. Scano, C. Thompson, Comparison of semiempirical MO methods applied to large molecules, J. Comput. Chem. 12 (1991) 172–174.
[37] Z.G. Soos, D.S. Galvão, One- and 2-photon excitations of polythiphene: role of nonconjugated heteroatoms, J. Phys. Chem. 98 (1994) 1029–1033, and references therein.
[38] D.S. Galvão, Z.G. Soos, S. Ramasesha, S. Etemad, A parametric method-3 (PM3) study of trans-stilbene, J. Chem. Phys. 98 (1993) 3016–3021.
[39] P.M.V.B. Barone, S.O. Dantas, D.S. Galvão, A semiempirical study on the electronic structure of ellipticines, J. Mol. Struct. (THEOCHEM) 465 (1999) 219–229.
[40] A. Koll, M. Rospenk, E. Jagodzinska, T. Dziembowska, Dipole moments and conformation of Schiff bases with intramolecular hydrogen bonds, J. Mol. Struct. 552 (2000) 193–204.
[41] H.F. dos Santos, W.B. de Almeida, MNDO/AM1/PM3 quantum mechanical semiempirical and molecular mechanics barriers to internal rotation: a comparative study, J. Mol. Struct. (THEOCHEM) 335 (1995) 129–139.
[42] V.V. Kislov, V.M. Petrov, S.Y. Noskov, V.N. Petrova, S.N. Ivanov, Molecular structure of *p*-methyl benzene sulphonyl halides and benzene sulphonyl chloride from quantum mechanical calculations and gas-phase electron diffraction, Internet J. Chem. 2 (9) (1999) 1–17.
[43] C.W. Jefford, G. Bernadinelli, M.C. Josso, P.Y. Morgantini, J. Weber, Comparative modeling studies on 3,6-substituted 1, 2, 4-trioxan-5-ones, J. Mol. Struct. (THEOCHEM) 337 (1995) 31–37.
[44] L. Gorb, A. Korkin, J. Leszczynski, A. Varnek, F. Mark, K. Schaffner, Theoretical ab initio and semiempirical studies on biologically important di- and oligopyrrolic compounds: pyrromethenone and biliverdin, J. Mol. Struct. (THEOCHEM) 425 (1998) 137–145.
[45] M.A. Palafox, F.J. Melendez, A comparative study of the scaled vibrational frequencies in the local anesthetics procaine, tetracaine and propoxycaine by means of semiempirical methods: AM1, PM3 and SAM1, J. Mol. Struct. (THEOCHEM) 459 (1999) 239–271.
[46] M.J.S. Dewar, E.F. Healy, A.J. Holder, Y.C. Yuan, Comments on a comparison of AM1 with the recently developed PM3 method, J. Comput. Chem. 11 (1990) 541.
[47] M. Cyrillo, D.S. Galvão, Chem2Pac: a Computational Chemistry Integrator for Windows, EPA Newsletter 67 (1999) 31–38. http://www.ifi.unicamp.br/gsonm/chem2pac.
[48] P.M.V.B. Barone, A. Camilo, D.S. Galvão, Theoretical approach to identify carcinogenic activity of polycyclic aromatic hydrocarbons, Phys. Rev. Lett. 77 (1996) 1186–1189.
[49] P.M.V.B. Barone, R.S. Braga, A. Camilo, D.S. Galvão, Electronic indices from semi-empirical calculations to identify carcinogenic activity of polycyclic aromatic hydrocarbons, J. Mol. Struct. (THEOCHEM) 505 (2000) 55–66.
[50] I.N. Levine, Quantum Chemistry, 4th Edition, Prentice-Hall, Englewood Cliffs, NJ, 1991.
[51] R. Vendrame, R.S. Braga, Y. Takahata, D.S. Galvão, Structure-activity relationship studies of carcinogenic activity of polycyclic aromatic hydrocarbons using calculated molecular descriptors with principal component analysis and neural network methods, J. Chem. Inf. Comput. Sci. 39 (1999) 1094–1104.
[52] L.L.D. Santo, D.S. Galvão, Structure-activity study of indolequinones bioreductive alkylating agents, J. Mol. Struc. (THEOCHEM) 464 (1999) 273–279.
[53] R. Vendrame, R.S. Braga, D.S. Galvão, Structure-activity relationship (SAR) studies of the tripos benchmark steroids, J. Chem. Inf. Comput. Sci., to be published.
[54] R.S. Braga, R. Vendrame, D.S. Galvão, Structure-activity relationship studies of substituted 17 alpha-acetoxyprogesterone hormones, J. Chem Inf. Comput. Sci. 40 (2000) 1377–1385.
[55] M. Cyrillo, D.S. Galvão, Structure-activity relationship study of some inhibitors of HIV-1 integrase, J. Mol. Struct. (THEOCHEM) 464 (1999) 267–272.
[56] J. Ridley, M.C. Zerner, Triplet states via intermediate neglect of differential overlap benzene, pyridine and diazines, Theo. Chim. Acta 42 (1976) 223–236.
[57] W.D. Edwards, M.C. Zerner, A generalized restricted open-shell Fock operator, Theo. Chim. Acta 72 (1987) 347–361.
[58] L.E. Bolívar-Marinez, M.C. dos Santos, D.S. Galvão, Electronic structure of push–pull molecules based on thiophene oligomers, J. Phys. Chem. 106 (1996) 11029–11032.
[59] L.E. Bolívar-Marinez, D.S. Galvão, M.J. Caldas, Geometric and spectroscopic study of some molecules related to eumelanins. Part 1. Monomers, J. Phys. Chem. B103 (1999) 2993–3000.
[60] Q. Gao, J. Golik, 2′-Carbamate taxol, Acta Cryst. C51 (1995) 2995–2998.
[61] Q. Gao, W.L. Parker, The hydrophobic collapse conformation of paclitaxel (Taxol®) has been observed in a non-aqueous environment: crystal structure of 10-deacetyl-7-epitaxol, Tetrahedron 52 (1996) 2291–2300.
[62] Q. Gao, S.-H. Chen, An unprecedented side chain conformation of paclitaxel (Taxol®): crystal structure of 7-mesylpaclitaxel, Tetrahedron Lett. 37 (1996) 3425–3428.
[63] D. Mastropaolo, A. Camerman, Y. Luo, G.D. Brayer, N. Camerman, Crystal and molecular structure of paclitaxel (taxol), Proc. Natl. Acad. Sci. U.S.A. 92 (1995) 6920–6924.
[64] J. Dubois, D. Guénard, F. Guérrite-Voegelein, N. Guedira, P. Potier, B. Gillet, J.-C. Beloeil, Conformation of Taxotere® and analogues determined by NMR spectroscopy and molecular modeling studies, Tetrahedron 49 (1993) 6533–6544.
[65] Y. Li, B. Poliks, L. Cegelski, M. Piloks, Z. Gryczynski, G. Piszczek, P.G. Jagtap, D.R. Studelska, D.G.I. Kingston, J. Scaefer, S. Bane, Conformation of microtubule-bound paclitaxel determined by fluorescence spectroscopy and REDOR NMR, Biochemistry 39 (2000) 281–291.
[66] M. Wang, B. Cornett, J. Nettles, D.C. Liotta, J.P. Snyder, The oxetane ring in taxol, J. Org. Chem. 65 (2000) 1059.
[67] B. Lythgoe, in: R.H.F. Manske (Ed.), The Alkaloids, Vol. 10, Academic Press, New York, 1968, p. 597.
[68] V. Farina (Ed.), The Chemistry and Pharmacology of Taxol® and its Derivatives, Elsevier, New York, 1995.
[69] S.F. Braga, D.S. Galvão, Structure-activity studies (SAR) of taxol and some derivatives using electronic indices methodology (EIM) and principal component analysis (PCA), to be published.